Supporting Information

Iron "Nano-Fishnet" for Rapid Removal and Surface Clean-up of Micro/nanoplastics from Seawater

Yufei Zhang[a], Zhiqiang Dong[b, c], Zilong Deng[b], Shuaiyi Shi[a], Chenliu Tang[a, *], Xiang Hu[a]

[a]Research Group of Water Pollution Control and Water Reclamation, College of Chemical Engineering, Beijing University of Chemical Technology, Beijing 100029, P.R. China

[b]College of Environmental Science and Engineering, Tongji University, Shanghai, 200092, P.R. China

[c]China Railway Engineering Group Co., Beijing 100039, P.R. China

*Corresponding author: **Chenliu Tang** (email: tangchenliu@buct.edu.cn; phone: +86-15800931374)

Table S1 Comparison of different physical strategies for micro/nanoplastics (MNPs) removal.

Removal Mechanism	Removal Technology	Aquatic environment	Type and size of plastics	MNPs removal efficiency	MNPs removal capacity	Reaction time	Ref.
Adsorption	Alkylated nanoscale zero-valent iron growing on the cellulose nanofibers (ac-nZVI) (This work)	Artificial Seawater (ASW)	10 μm PS, PVC, PMMA	95.71% (PS) 97.64% (PVC) 94.97% (PMMA)	324.88 mg_{MNPs} g_{Fe}^{-1} (PS) 278.99 mg_{MNPs} g_{Fe}^{-1} (PVC) 267.71 mg_{MNPs} g_{Fe}^{-1} (PMMA)	1 min	/
			2 μm PS, PVC, PMMA	97.47% (PS) 98.58% (PVC) 95.10% (PMMA)	141.50 mg_{MNPs} g_{Fe}^{-1} (PS) 179.01 mg_{MNPs} g_{Fe}^{-1} (PVC) 167.62 mg_{MNPs} g_{Fe}^{-1} (PMMA)		
	Hydrophobic Fe nanoparticles	Seawater	100 nm PS	98.28%	40.96 mg_{MNPs}/g_{Fe}	Mix for 5 min and magnetic recover for 30 min	[1]
			10-20 μm PE and PS beads	92%	/		
			>1 mm MPs (PE, PS, PU, PET, etc.)	92%			
		Freshwater	200 μm– 1 mm (PE, PS, PU, PVC, etc.)	84%			
	Oat protein sponges	DI water (pH=6~9, 25 °C)	1 μm PS	≤81.2%	5.7 mg L^{-1}	24 h	[2]
	Chitin-based sponge (ChCN, ChGO, and ChGO-CT)	DI water (pH=6~8, 45 °C)	1 μm PS	89.6-92.1%	9.67 mg L^{-1} (ChGO)	48 h	[3]
			1 μm PS-COOH	80.4-81.3%	8.86 mg L^{-1} (ChGO)		
			1 μm PS-NH_2	83.2-87.1%	12.9 mg L^{-1} (ChCN)		
	Biochar and modified biochar	DI water (25 °C)	1 μm PS	94.81%	100.6 mg g^{-1} (MBCs)	5 h	[4]
				98.75%	98.52 mg g^{-1}		

				99.46%	(Mg-MBCs) 99.21 mg g^{-1} (Zn-MBCs)		
	Photocatalytic TiO_2-based Micromotor (Au@mag@TiO_2, mag=Ni, Fe)	DI water	Extracts from toothpaste, washing powder, face cleansing cream, and Baltic Sea	67-71%	/	24 h	[5]
	Ppolydopamine (PDA)@Fe_3O_4 magnetic microrobots (MagRobots)	DI water	rubbing the surface of a 50 mL plastic centrifuge tube with a nail file	/	/	/	[6]
	$BiVO_4/Fe_3O_4$ microrobots	DI water (0.01-0.1 wt % H_2O_2)	PLA, PCL, PET, PP (100-200 μm)	10-70%	/	/	[7]
Coagulation	$FeCl_3$	DI water	PS, PE (< 500 μm)	~18.0-~62.0%	/	~46 min	[8]
	PAC		PS, PE (< 500 μm)	29.7-77.8%			
	$AlCl_3$, $Al_2(SO_4)_3$, $FeCl_3$, $CH_3(CH_2)_3SiCl_3$, and $CH_3(CH_2)_7SiCl_3$	Simulated seawater	PBMA (200-1500 μm)	>60%	/	24 h	[9]
Filtration	Biochar sand filter	Distilled water (pH=7.56)	PS (10 μm)	>95%	/	~4 h	[10]

Table S2 Nature of real seawater.

Chemical indicators	Bo Hai	Yellow Sea	East China Sea	North China Sea
pH	7.33	7.88	8.14	8.03
Salinity (g/kg)	27.89	30.46	31.84	33.84
Total organic carbon (TOC, mg/L)	2.19	2.04	2.31	2.27
Na^+ (g/L)	9.80	10.78	11.39	11.96
K^+ (mg/L)	357.20	352.40	390.60	404.60
Ca^{2+} (mg/L)	389.70	372.30	401.90	417.20
Mg^{2+} (g/L)	1.19	1.34	1.40	1.48
Cl^- (g/L)	18.21	21.89	23.45	25.14
SO_4^{2-} (g/L)	1.34	1.27	1.26	1.24

Table S3 Fe concentration in supernatant after ac-nZVI reaction with different MNPs in ASW.

Types of MNPs	Fe^{2+}/Fe^{3+} concentration (ppm)		
	100 nm	2 μm	10 μm
PS	0.49±0.03	0.45±0.02	0.53±0.06
PVC	-	0.51±0.05	0.47±0.02
PMMA	-	0.71±0.14	0.56±0.01

Table S4 XPS Fe 2p concentration (atomic%) of nZVI and ac-nZVI.

Materials	Fe^0	Fe^{2+}	Fe^{3+}
nZVI	12.65	51.18	36.16
ac-nZVI	36.30	22.49	41.23

Table S5 Calculated collection capability of ac-nZVI for different MNPs in ASW.

Types of MNPs	Calculated collection capability (10^8 pcs/g_{Fe})		
	100 nm	2 μm	10 μm
PS	84559.00±6600.33	450.08±6.08	6.46±1.94
PVC	-	358.01±18.03	5.30±0.10
PMMA	-	335.25±14.96	5.09±0.68

Table S6 The remaining Pb^{2+} concentration in MNPs-Pb(II) solution after reacting with ac-nZVI at 1 h, 2 h, 6 h and 12 h.

Reaction time	1 h	2 h	6 h	12 h
Pb^{2+} concentration (ppb)	BDL	BDL	BDL	BDL

BDL means below detection limit.

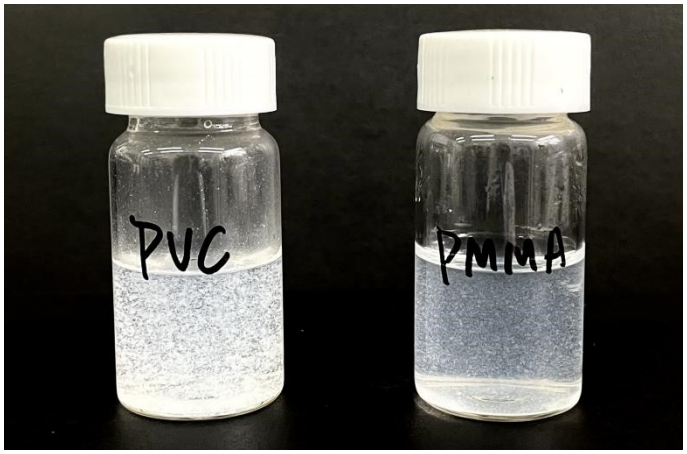

Fig. S1 100 nm PVC MNPs and 100 nm PMMA MNPs dispersed in ASW.

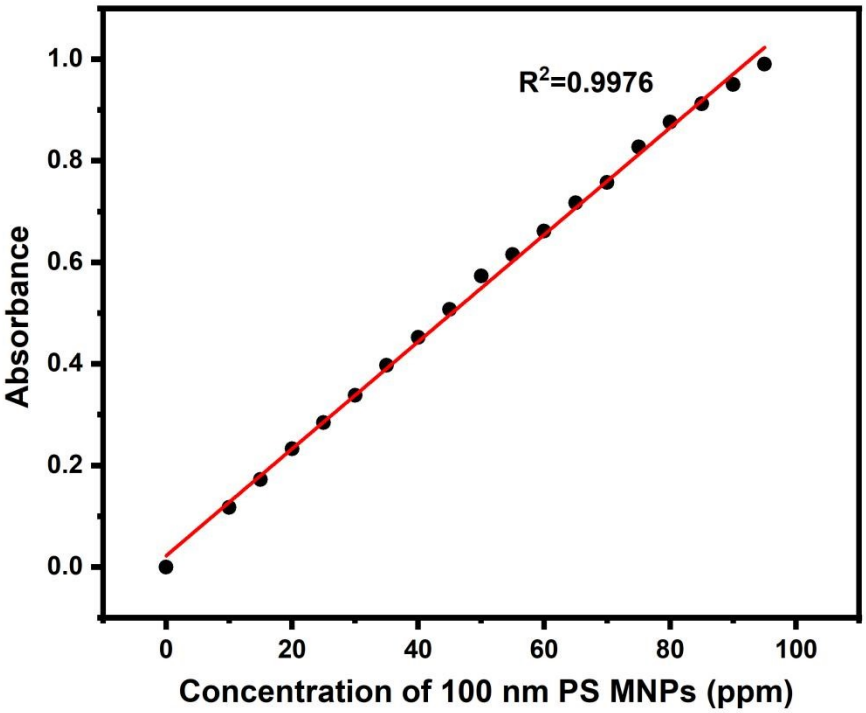

Fig. S2 Calibration curve of absorbance for 100 nm PS MNPs.

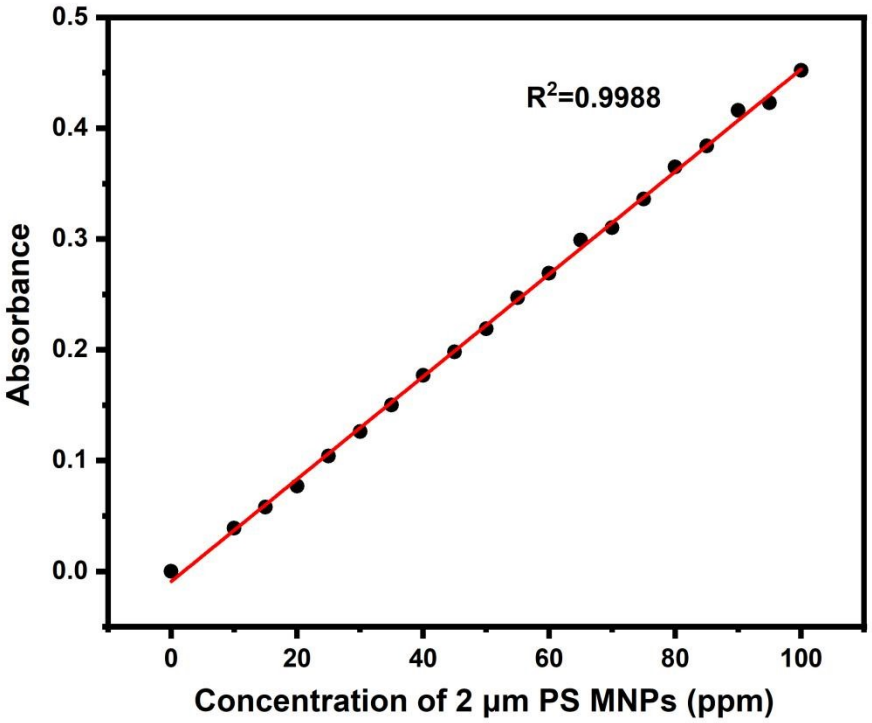

Fig. S3 Calibration curve of absorbance for 2 μm PS MNPs.

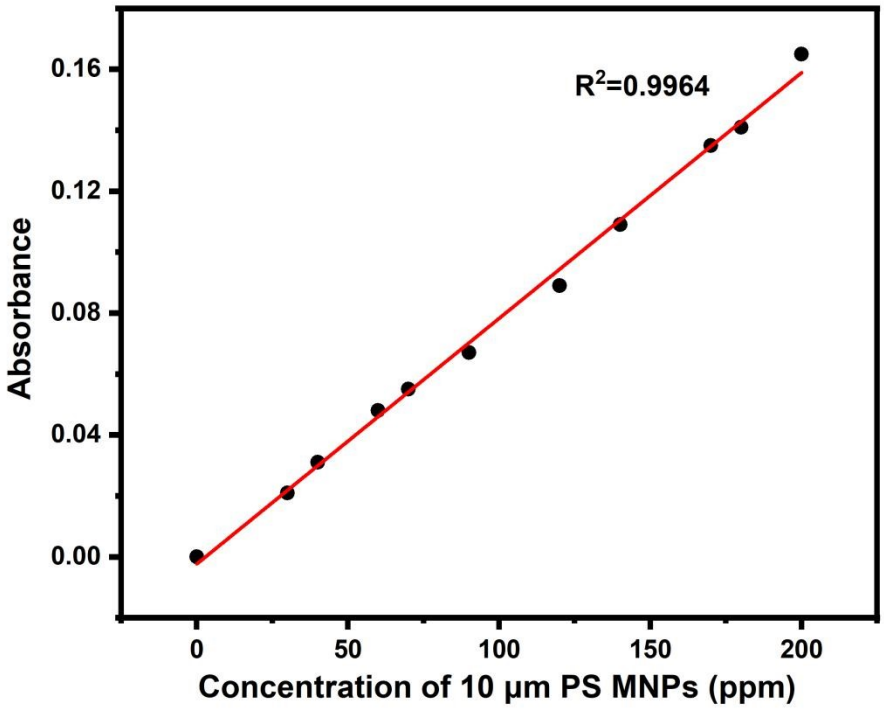

Fig. S4 Calibration curve of absorbance for 10 μm PS MNPs.

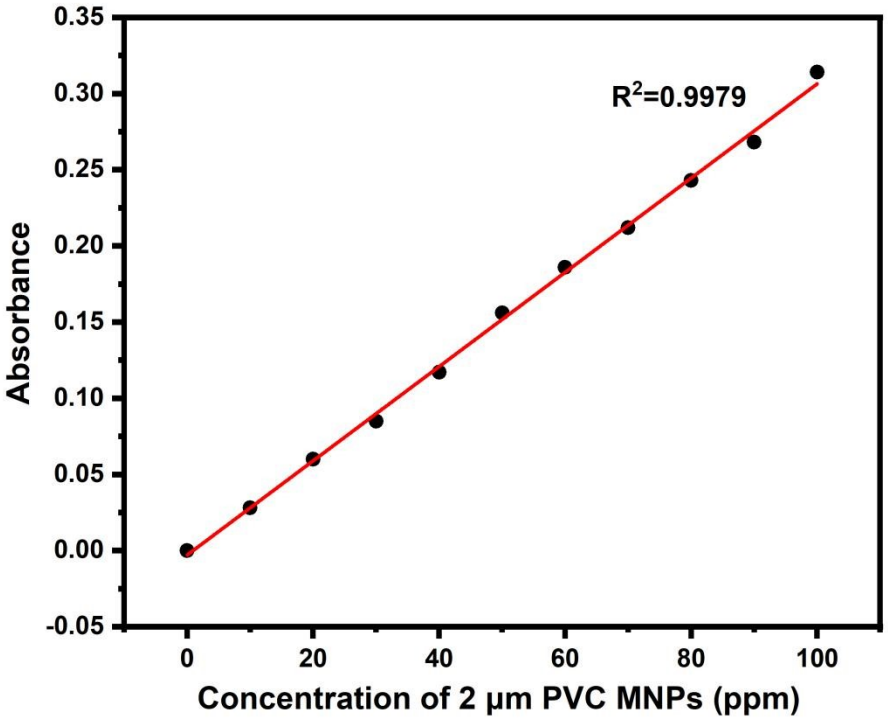

Fig. S5 Calibration curve of absorbance for 2 µm PVC MNPs.

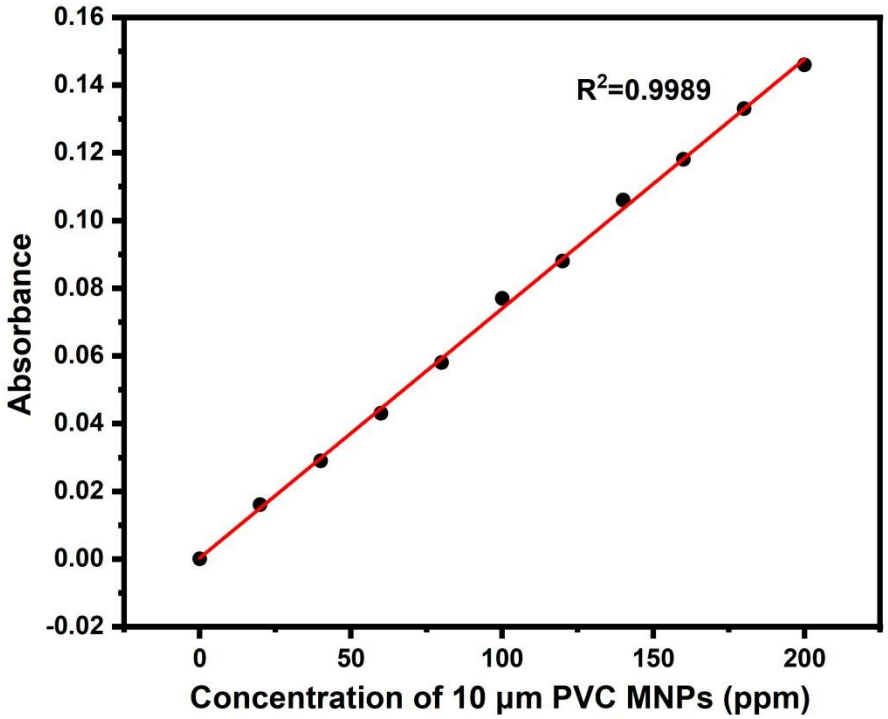

Fig. S6 Calibration curve of absorbance for 10 µm PVC MNPs.

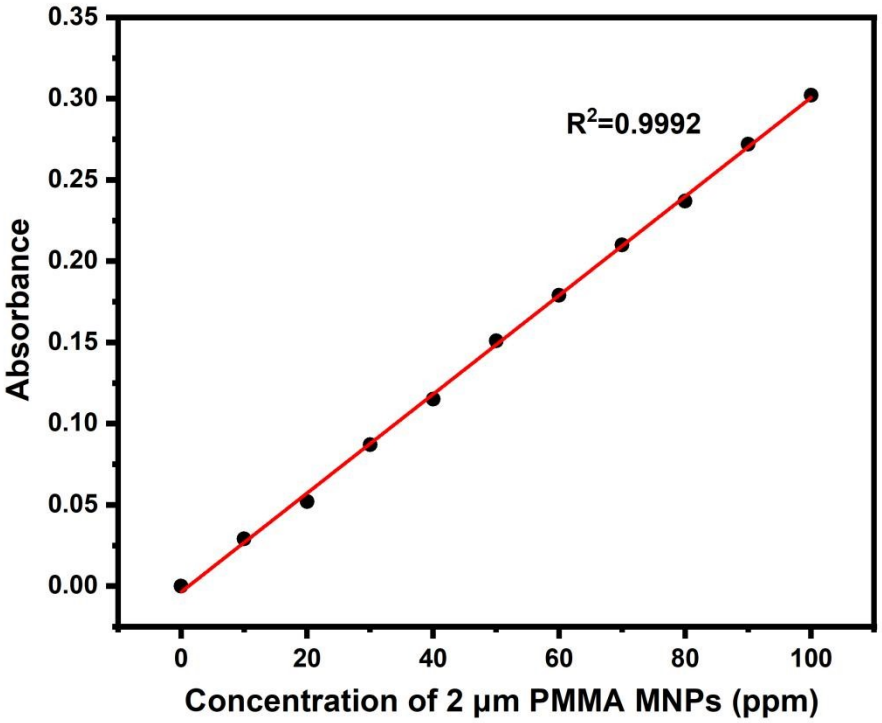

Fig. S7 Calibration curve of absorbance for 2 μm PMMA MNPs.

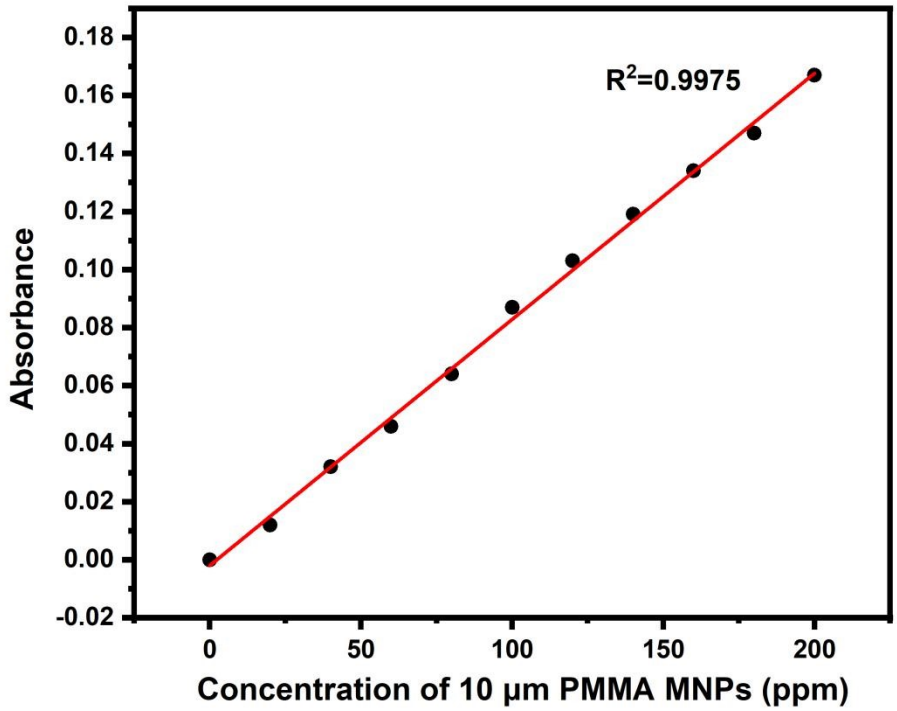

Fig. S8 Calibration curve of absorbance for 10 µm PMMA MNPs.

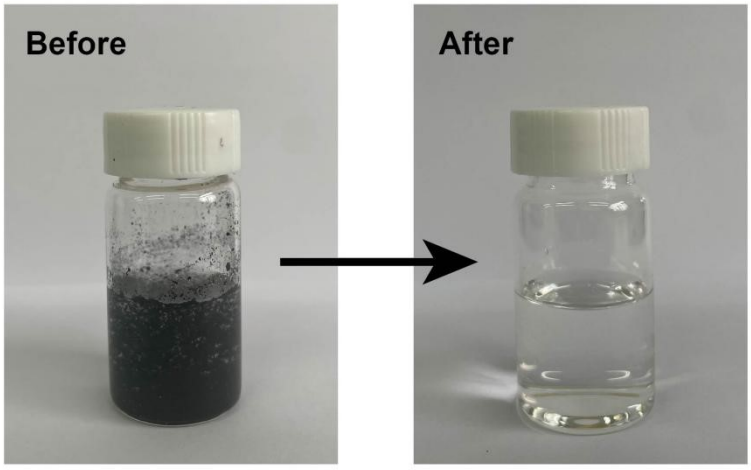

Fig. S9 Images of magnetic separation of ac-nZVI from ASW. After magnetic recovery, the absorbance of the supernatant was clear and close to that of ASW, that was, the change in absorbance mainly originated from the variations of MNPs concentration.

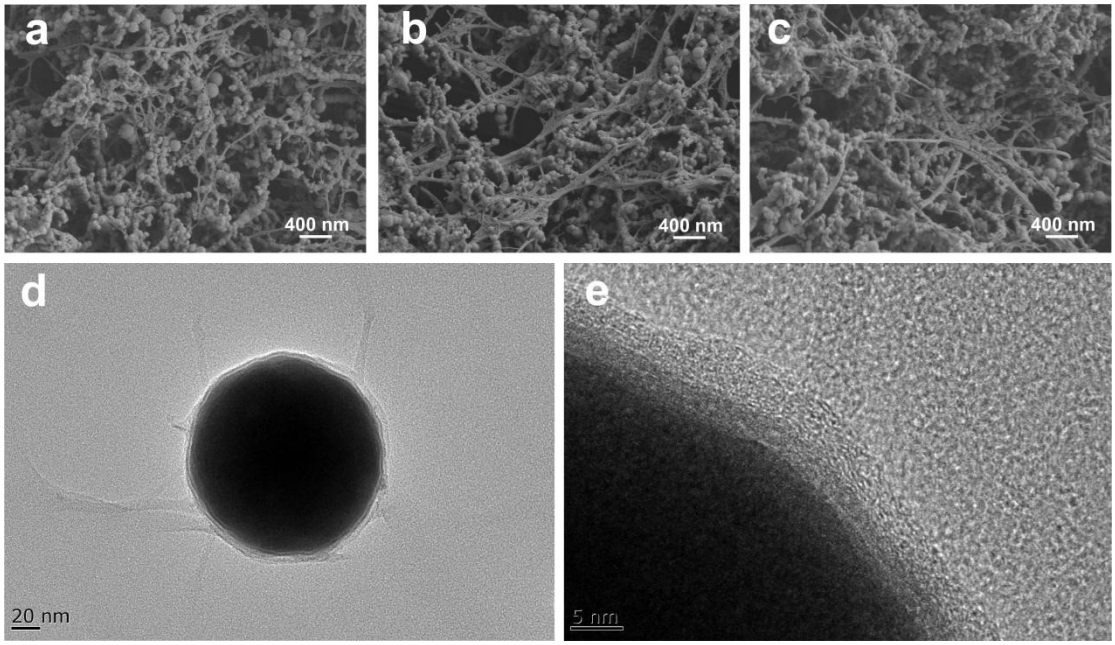

Fig. S10 (a)-(c) SEM images and (d)-(e) TEM images of ac-nZVI.

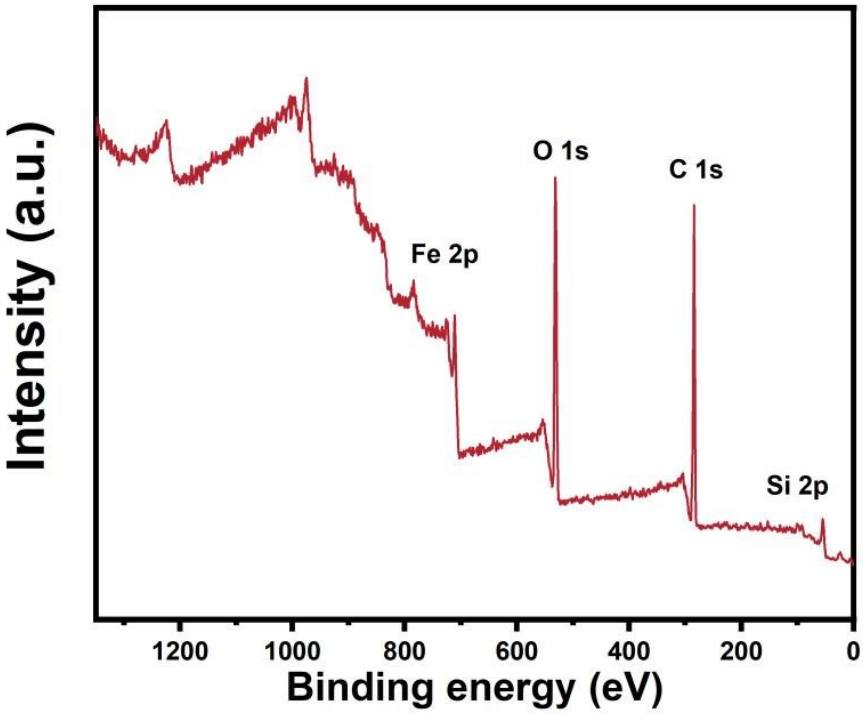

Fig. S11 XPS survey of ac-nZVI.

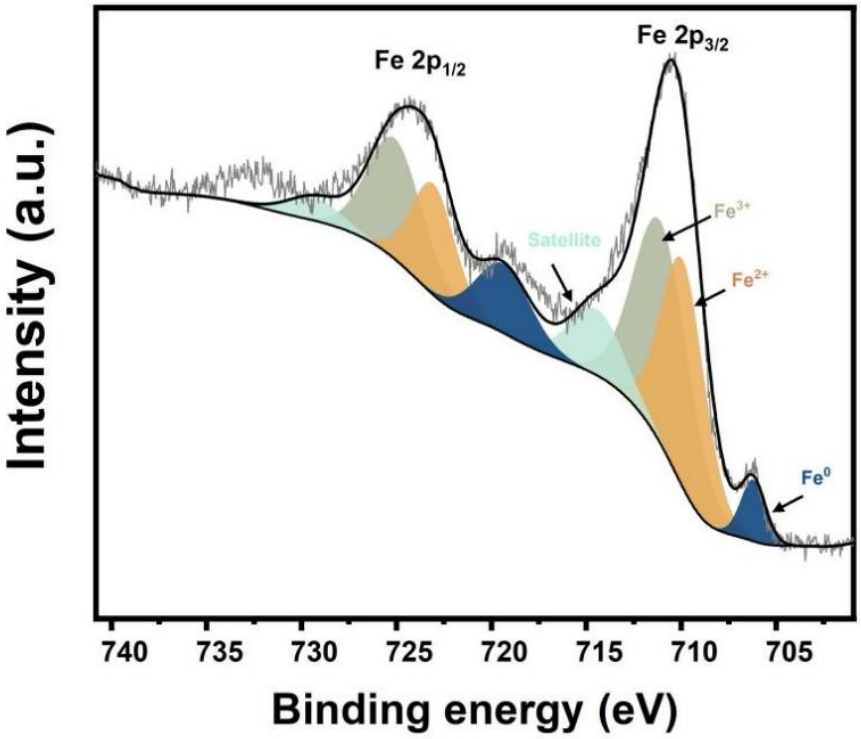

Fig. S12 XPS Fe 2p fine spectrum of nZVI.

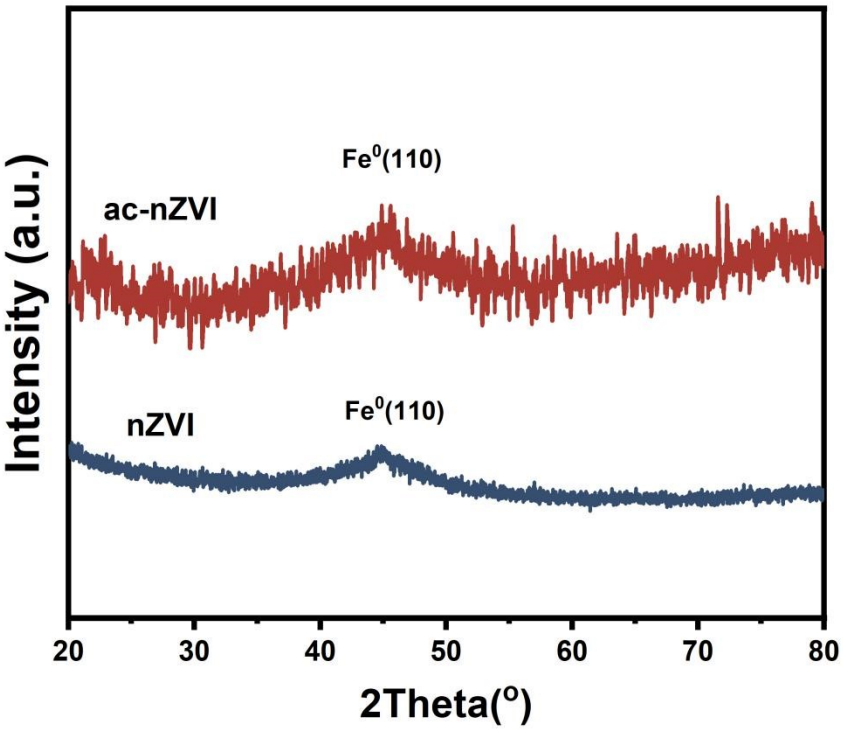

Fig. S13 XRD patterns of nZVI and ac-nZVI.

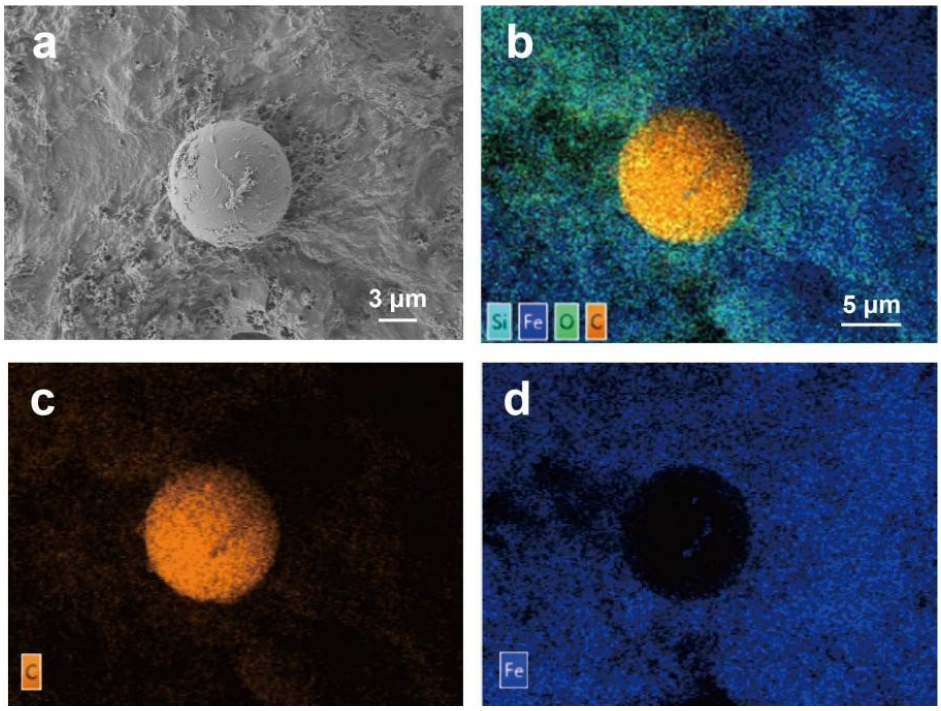

Fig. S14 (a) SEM image; (b)-(d) EDS mapping of 10 µm PS MNPs removed by ac-nZVI. Conditions: MNPs concentration = 100 mg/L (ASW, initial pH = 8), ac-nZVI dosage = 1 g/L, reaction time = 1 min, T = 25°C.

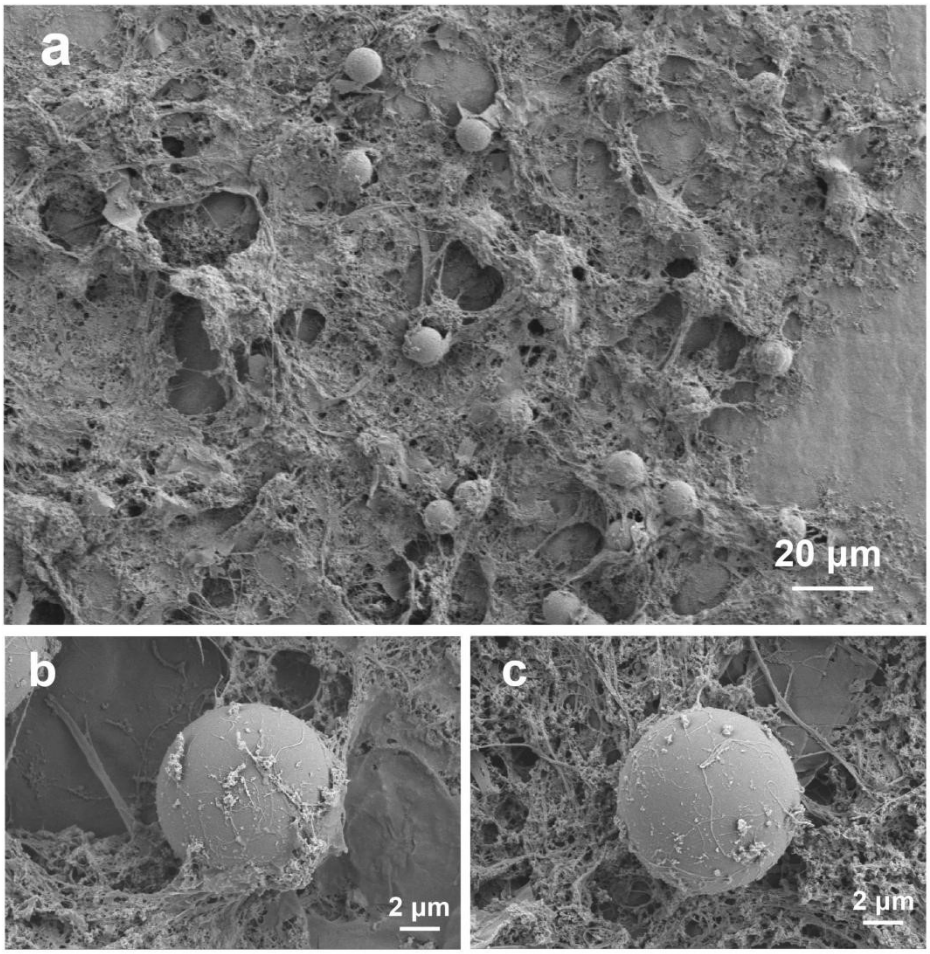

Fig. S15 (a)-(c) SEM images of 10 μm PVC MNPs removed by ac-nZVI. Conditions: MNPs concentration = 100 mg/L (ASW, initial pH = 8), ac-nZVI dosage = 1 g/L, reaction time = 1 min, T = 25°C.

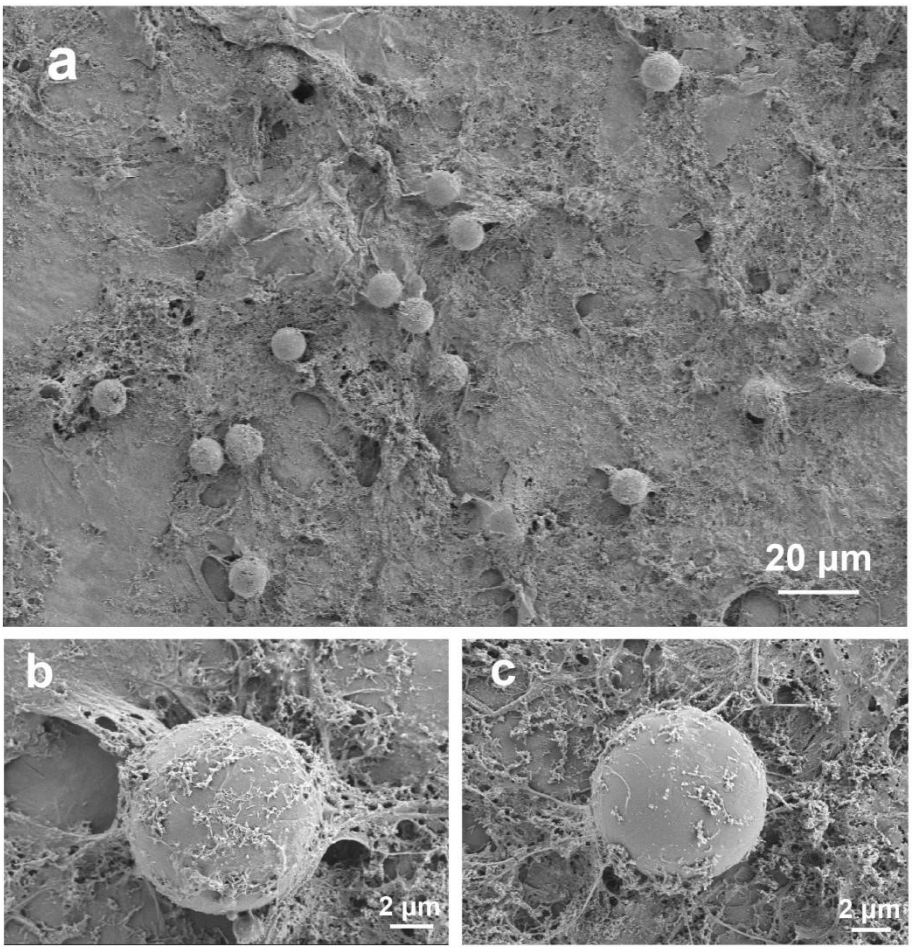

Fig. S16 (a)-(c) SEM images of 10 µm PMMA MNPs removed by ac-nZVI. Conditions: MNPs concentration = 100 mg/L (ASW, initial pH = 8), ac-nZVI dosage = 1 g/L, reaction time = 1 min, T = 25°C.

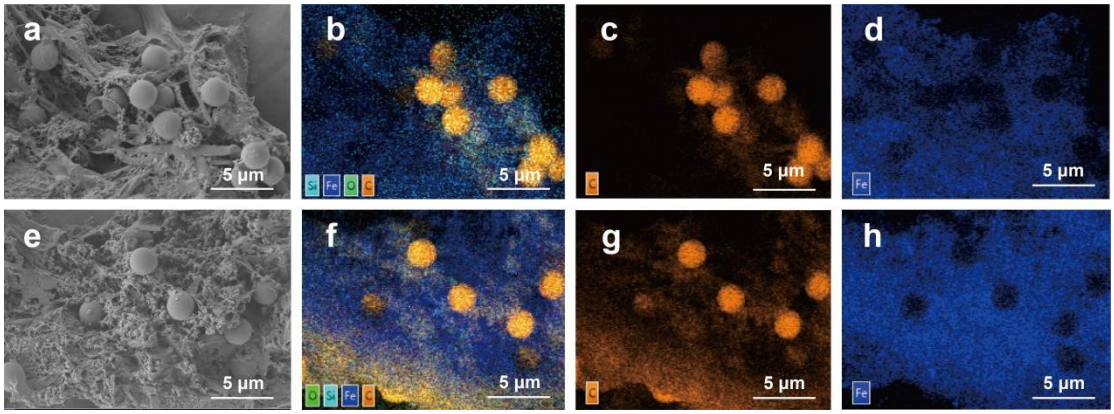

Fig. S17 (a) and (e) SEM images; (b)-(d) and (f)-(h) EDS mapping of 2 μm PS MNPs removed by ac-nZVI. Conditions: MNPs concentration = 100 mg/L (ASW, initial pH = 8), ac-nZVI dosage = 1 g/L, reaction time = 1 min, T = 25℃.

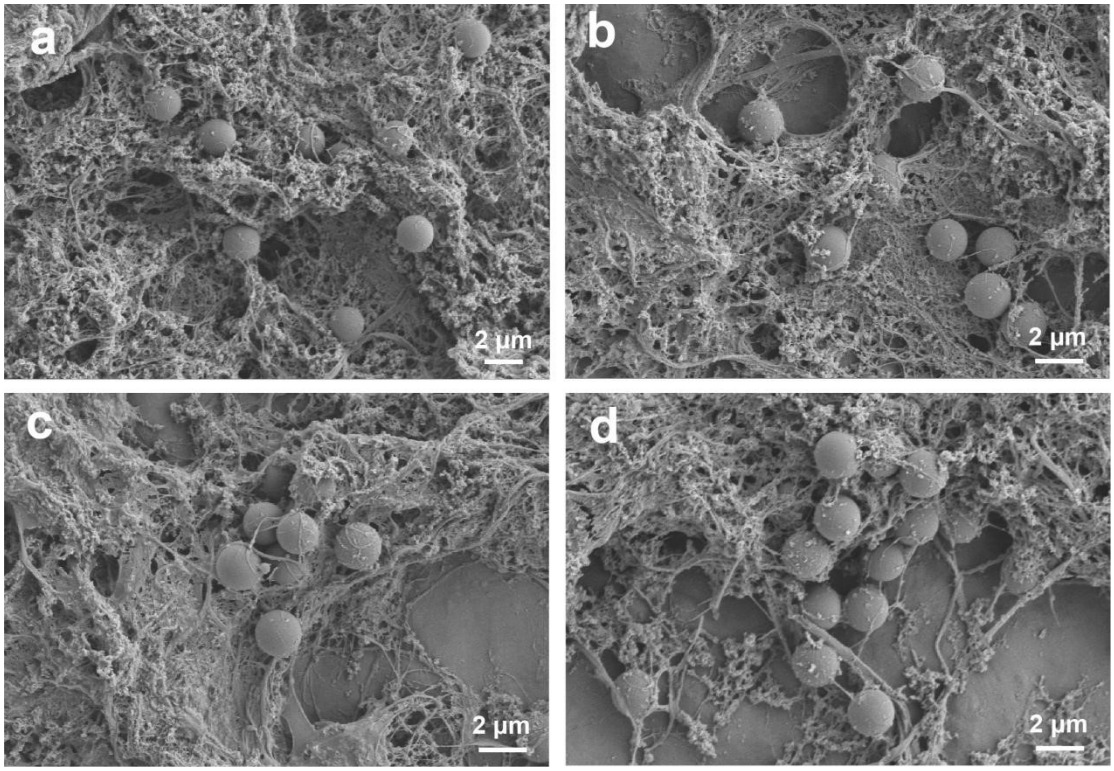

Fig. S18 (a)-(d) SEM images of 2 μm PVC MNPs removed by ac-nZVI. Conditions: MNPs concentration = 100 mg/L (ASW, initial pH = 8), ac-nZVI dosage = 1 g/L, reaction time = 1 min, T = 25°C.

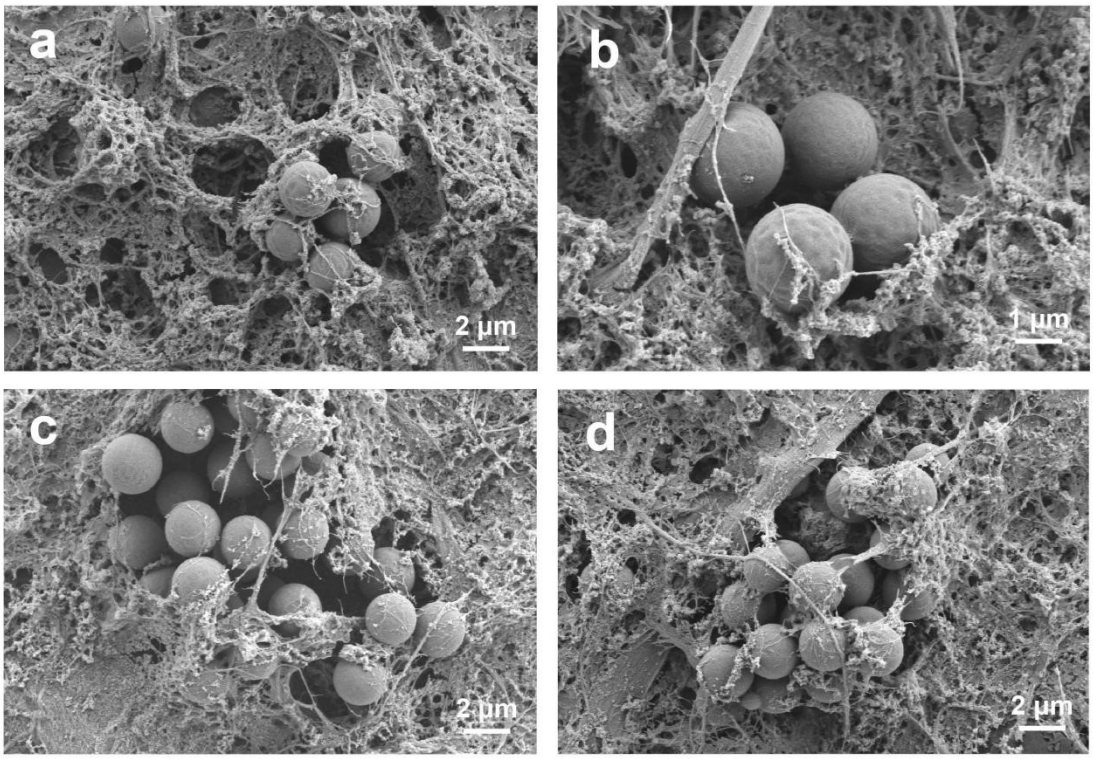

Fig. S19 (a)-(d) SEM images of 2 μm PMMA MNPs removed by ac-nZVI. Conditions: MNPs concentration = 100 mg/L (ASW, initial pH = 8), ac-nZVI dosage = 1 g/L, reaction time = 1 min, T = 25°C.

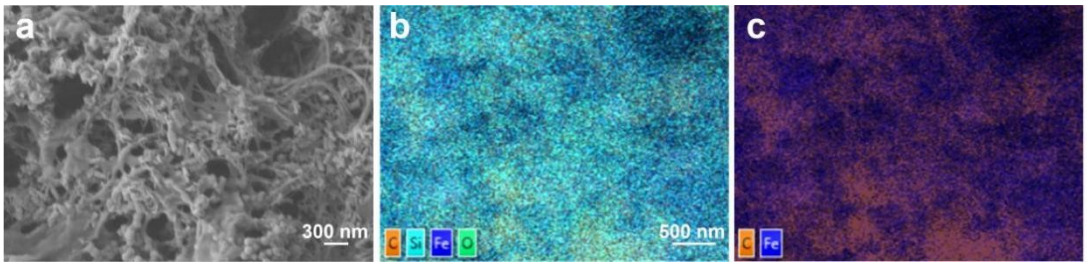

Fig. S20 (a) SEM image; (b) and (c) EDS mapping of 100 nm PS MNPs removed by ac-nZVI. Conditions: MNPs concentration = 100 mg/L (ASW, initial pH = 8), ac-nZVI dosage =1 g/L, reaction time = 1 min, T = 25℃.

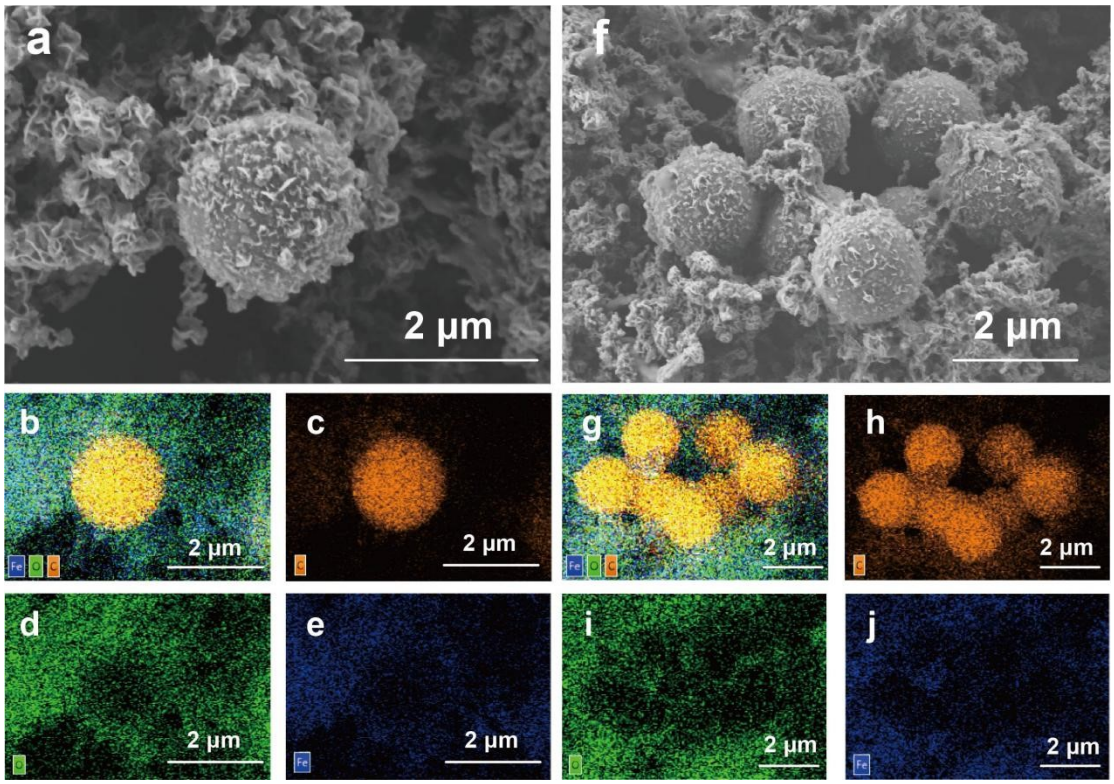

Fig. S21 (a) and (f) SEM images; (b)-(e) and (g)-(j) EDS mapping of 2 μm MNPs removed by nZVI. Conditions: MNPs concentration = 100 mg/L (ASW, initial pH = 8), nZVI dosage = 1 g/L, reaction time = 1 min, T = 25°C.

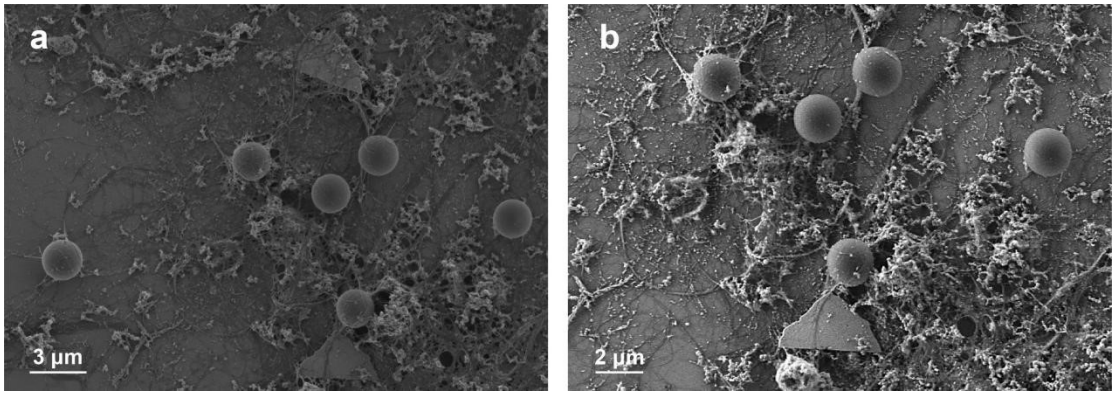

Fig. S22 (a) and (b) SEM images of 2 µm MNPs-Pb(II) reacting with ac-nZVI. Conditions: MNPs initial concentration = 10 mg/L (ASW, initial pH = 8), ac-nZVI dosage = 0.5 g/L, T = 25°C.

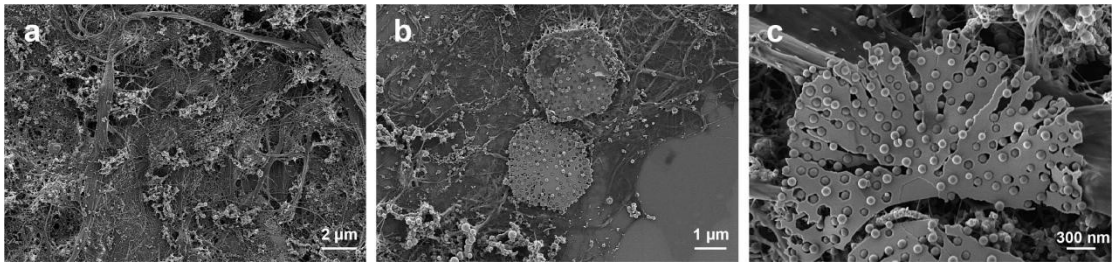

Fig. S23 (a)-(c) SEM images of 100 nm MNPs-Pb(II) reacting with ac-nZVI. Conditions: MNPs initial concentration = 10 mg/L (ASW, initial pH = 8), ac-nZVI dosage = 0.5 g/L, T = 25℃. Similar polygon flakes are formed on the netting wires of ac-nZVI. 100 nm MNPs participate in the formation of lead products, breaking and embedding into the nanoplate structure.

Video S1-S3 The procedure of 10 μm, 2 μm, 100 nm PS MNPs removal with ac-nZVI, respectively.

References

1 J. Grbic, B. Nguyen, E. Guo, J. B. You, D. Sinton and C. M. Rochman, Magnetic Extraction of Microplastics from Environmental Samples, *Environ. Sci. Technol. Lett*., 2019, **6**, 68–72.

2 Z. Wang, C. Sun, F. Li and L. Chen, Fatigue Resistance, Re-Usable and Biodegradable Sponge Materials from Plant Protein with Rapid Water Adsorption Capacity for Microplastics Removal, *Chem. Eng. J*., 2021, **415**, 129006.

3 C. Sun, Z. Wang, H. Zheng, L. Chen and F. Li, Biodegradable and Re-Usable Sponge Materials Made from Chitin for Efficient Removal of Microplastics, *J. Hazard. Mater.*, 2021, **420**, 126599.

4 J. Wang, C. Sun, Q.-X. Huang, Y. Chi and J.-H. Yan, Adsorption and Thermal Degradation of Microplastics from Aqueous Solutions by Mg/Zn Modified Magnetic Biochars, *J. Hazard. Mater.*, 2021, **419**, 126486.

5 L. Wang, A. Kaeppler, D. Fischer and J. Simmchen, Photocatalytic TiO_2 Micromotors for Removal of Microplastics and Suspended Matter, *ACS Appl. Mater. Interfaces*, 2019, **11**, 32937–32944.

6 H. Zhou, C. C. Mayorga-Martinez and M. Pumera, Microplastic Removal and Degradation by Mussel-Inspired Adhesive Magnetic/Enzymatic Microrobots, *Small Methods*, 2021, **5**, 2100230.

7 S. M. Beladi-Mousavi, S. Hermanová, Y. Ying, J. Plutnar and M. Pumera, A Maze in Plastic Wastes: Autonomous Motile Photocatalytic Microrobots against Microplastics, *ACS Appl. Mater. Interfaces*, 2021, **13**, 25102–25110.

8 G. Zhou, Q. Wang, J. Li, Q. Li, H. Xu, Q. Ye, Y. Wang, S. Shu and J. Zhang, Removal of Polystyrene and Polyethylene Microplastics Using PAC and $FeCl_3$ Coagulation: Performance and Mechanism, *Sci. Total Environ*., 2021, **752**, 141837.

9 P. S. Lee and S. M. Jung, Quantitative Analysis of Microplastics Coagulation-Removal Process for Clean Sea Salt Production, *Int. J. Environ. Sci. Technol*.,

2022, **19**, 5205–5216.

10 Z. Wang, M. Sedighi and A. Lea-Langton, Filtration of Microplastic Spheres by Biochar: Removal Efficiency and Immobilisation Mechanisms, *Water Res*., 2020, **184**, 116165.